Nuclear Physics A548 (1992) 365–373
North-Holland

NUCLEAR
PHYSICS A

Photofission and photoneutron measurements on ^{241}Am between 5 and 10 MeV

S.J. Watson[1], D.J.S. Findlay and M.R. Sené
Harwell Laboratory, UKAEA, Oxfordshire OX11 0RA, UK

Received 8 April 1992

Abstract: Measurements are presented of the photofission and photoneutron cross sections of ^{241}Am and of the mean number $\bar{\nu}$ of neutrons per fission between 5 and 10 MeV. The measurements were carried out using a bremsstrahlung beam generated by the Harwell electron linear accelerator HELIOS and a 1.5 g metallic ^{241}Am target. Neutron multiplicity distributions were recorded using a high-efficiency neutron detector. Yield measurements made in steps of 50 keV show possible evidence for a resonance at 6.1 MeV in the photofission cross section, but the statistical significance is not high.

E | NUCLEAR REACTIONS ^{241}Am(γ, F), ^{241}Am(γ, n), $E = 5.6$–10 MeV; measured photon induced $\sigma(E)$; deduced photofission, photoneutron σ, mean number of neutrons per fission. ^{241}Am deduced fission characteristics.

1. Introduction

Photofission has been used extensively in the study of actinide fission near threshold due to the relatively small number of low-lying states excited by the predominantly E1 interaction. Near threshold most excitation energy is converted into nuclear deformation energy, and so fission proceeds through only a few low-lying fission channels. This makes interpretation of experimentally measured cross sections easier for fission induced by photons than fission induced by other particles (e.g. neutrons) [1]).

In photofission experiments there has tended to be an emphasis on actinide nuclei such as even-even ^{232}Th and ^{238}U for which suitable targets are readily obtainable. A comprehensive reference list for such experiments is included in ref. [2]). There have been fewer experimental photofission studies of heavier nuclei, and in particular of the heavier odd-A nuclei [3–7]).

Photofission of the odd-A nucleus ^{241}Am has been studied only by Zhuchko *et al.* [3]) and Koretskaya *et al.* [4]). Zhuchko *et al.* used bremsstrahlung to study the photofission cross section between 5 and 7 MeV with an energy resolution of

Correspondence to: Dr. D.J.S. Findlay, Accelerator Applications Department, AEA Technology Building 418, Harwell Laboratory, Oxfordshire OX11 0RA, UK.
[1] Energy Research Unit, Rutherford Appleton Laboratory, Oxfordshire OX11 0QX, UK.

~200-300 keV. Koretskaya *et al.* made measurements at 1 MeV intervals between 7 and 26 MeV. Measurements of the photoneutron cross section between 11 and 15 MeV have been made by Batij *et al.* [8]). The measurements for ^{241}Am in the photon energy range 5.6-10 MeV presented in this paper are intended to supplement existing data on ^{241}Am, and are of the photofission and photoneutron cross sections and the mean number $\bar{\nu}$ of prompt fission neutrons per fission.

2. The experiment

Measurements for this experiment were made on the electron linear accelerator HELIOS [9]) at the Harwell Laboratory of the UK Atomic Energy Authority. Only brief details of the experimental apparatus and procedures will be given here, since full details are given in ref. [10]).

After the second section of the accelerator, the electron beam was energy analysed by a magnetic analysis system incorporating a computer-controlled power supply locked to a Rawson-Lush rotating coil gaussmeter. Bremsstrahlung from a gold radiator was collimated and intercepted by the ^{241}Am target. Neutrons photoproduced from the target were detected in a large high-efficiency neutron detector consisting of an oil-moderated tank containing fifty-six $^{10}BF_3$ proportional counters arranged in five concentric rings (the neutron detection efficiency varied between 40% and 48% for neutron energies between 0.5 and 5 MeV). The bremsstrahlung flux was measured absolutely using a type P2 ionisation chamber [11]) connected to a Brookhaven model 1000A current integrator.

The ^{241}Am target itself was supplied by the Oak Ridge National Laboratory (USA) in the form of a square 2 × 2 cm metallic foil of mass 1.533 g and thickness 0.38 g cm^{-2} mounted between two thin (0.01 mm) nickel foils in an evacuated aluminium can 89 mm in diameter and 569 mm long with a 0.5 mm thick aluminium entrance window. Around the can was placed 2 mm of lead to attenuate the 60 keV γ-rays produced by the ~5 Ci target. The position of the target within the can was confirmed by autoradiography. The can had been evacuated to prevent oxidation of the highly α-active americium and hence avoid production of neutrons through the $^{16}O(\alpha, n)$ reaction. Unfortunately, upon receipt of the target it was found that the target was already emitting ~7500 neutrons/s. From γ-ray spectroscopy measurements, these neutrons were found to be due to the $^{19}F(\alpha, n)$ reaction implying that the target had been contaminated by fluorine which could have been a by-product of the original metal extraction process. The presence of the fluorine impurity had not been declared in the chemical analysis of the target. In the present experiment this large neutron background limited the minimum energy which could be reached.

Yields were measured at regularly spaced bremsstrahlung endpoint energies over the range of interest. Two sets of measurements were made at 100 keV intervals between 5.6 and 8.0 MeV, one set of measurements was made at 200 keV intervals between 8.0 and 10.0 MeV, and one set of measurements was made at 50 keV intervals

between 5.7 and 6.4 MeV. To minimise the effects of small systematic drifts in energy, yields were measured at two neighbouring energy points during each run and the energy was cycled between these points so that data were taken for 1 minute at each endpoint energy. The difference of the pair of yields from each run was then used as the input to the unfolding procedure described in sect. 3. To eliminate effects of drift in the zero of the P2 ionisation chamber and current integration system, especially at higher energies where the electron beam current had to be greatly reduced to keep the detected event rate at or below 0.1 events per beam burst, the integrator was operated with a permanently positive offset. Therefore between each minute's running, the electron beam was switched off for 10 seconds and the integrator output in the absence of beam was recorded.

3. Analysis

The raw data are sets of pairs of neutron multiplicity distributions, each pair corresponding to the two adjacent endpoint energies in each run. After correcting for background, dead time and overlap as described in ref. [12]), the sum and difference of each pair of multiplicity distributions was formed. The "sum" multiplicity distribution was fitted by the TRDG [13]) multiplicity-distribution shape to extract the parameters $\bar{\nu}$ and σ^2, the mean and variance respectively of the distribution. Assuming that changes in $\bar{\nu}$ and σ^2 between adjacent end point energies are relatively small, these values of $\bar{\nu}$ and σ^2 were then used for the "difference" multiplicity distribution to extract the numbers of photofission and photoneutron events corresponding to the difference multiplicity distribution. These "difference" yields were then taken as input to a modified Penfold-Leiss unfolding procedure [14]) re-cast in terms of yield differences [15]).

Between 5.6 and 8.0 MeV, two-fold interlacing* was used to reduce the statistical errors on the unfolded cross-section data points at the expense of energy resolution. Above 8 MeV, multiplicity-distribution shape parameters were measured every 500 keV, and these parameter values were used to extract photofission and photoneutron cross sections from the set of yield data points measured every 200 keV above 8 MeV.

4. Results

Fig. 1 shows the photofission cross sections from the present experiment. Also shown are the results of Zhuchko *et al.* [3]) and Koretskaya *et al.* [4]). Below 8 MeV the energy resolution of the present data is 220 keV, the 100 keV data being two-fold

* The set of yields at 100 keV intervals between 5.6 and 8.0 MeV was considered to be two sets of yields, one set at 200 keV intervals between 5.6 and 8.0 MeV, the other set at 200 keV intervals between 5.7 and 7.9 MeV. The two sets of yields were unfolded separately and the two sets of unfolded cross-section values were then combined to form one composite set.

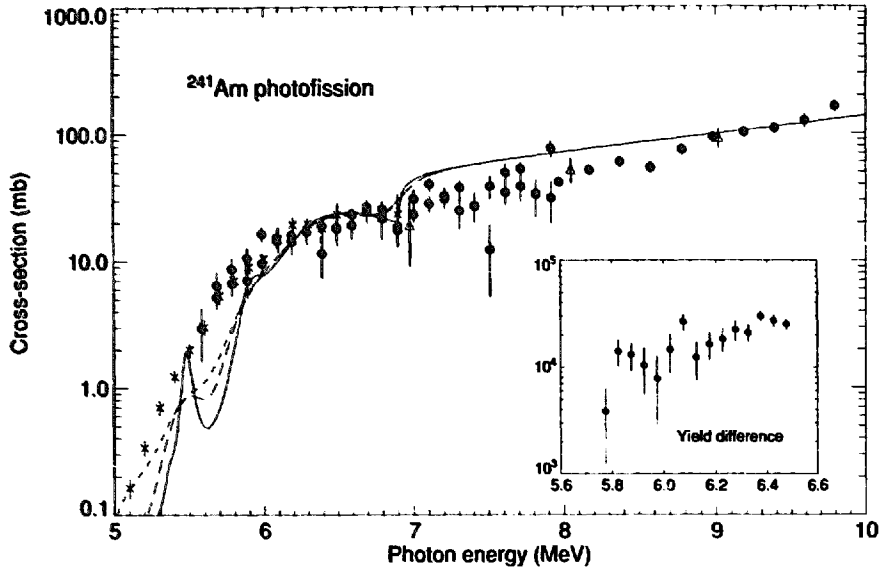

Fig. 1. Photofission cross section for ^{241}Am. Data: Solid circles, present measurements; crosses, Zhuchko *et al.* [3]); triangles, Koretskaya *et al.* [4]). Curves (as discussed in the text): solid line, no damping in second well; long dashes, as solid curve but including effects of 220 keV experimental energy resolution; short dashes, 300 keV damping in second well and 220 keV resolution. The inset shows the yield differences (counts μC^{-1}).

interlaced, and above 8 MeV the energy resolution is 500 keV. The Zhuchko *et al.* data has a resolution of between 200 and 300 keV. The present data agree well with those of Zhuchko *et al.* In the inset to fig. 1 are shown yield differences from the 50 keV measurements between 5.7 and 6.4 MeV where the energy "resolution" is ~50 keV. It is possible that there is a resonant-like structure at 6.1 MeV, but the statistical significance is not high. Further high-resolution measurements in this energy region might help to establish whether any structure actually does exist.

In fig. 2 is shown a comparison of the fissilities from the present experiment with those of Back *et al.* [16]) for the ^{240}Pu(^{3}He, df)^{241}Am reaction. The fissility P_f is given by

$$P_f = \frac{\sigma_f}{\sum_i \sigma_i}, \tag{1}$$

where the numerator is the fission cross section and the denominator is the total-reaction cross section given by the sum of all the individual reaction cross sections i. For the present data, the denominator of eq. (1) was approximated by a two-lorentzian representation of the total-absorption cross section with parameters [3]) averaged over the actinides. Also shown in fig. 2 are fissilities obtained from the cross sections of Zhuchko *et al.* in the same way. In spite of the differences in spin distributions produced by the charged particle and photonuclear interactions, the fissilities are very similar. This is presumably due to the relatively large range of spin states reached by the photonuclear interaction from the non-zero $\frac{5}{2}^-$ ground-state spin of ^{241}Am.

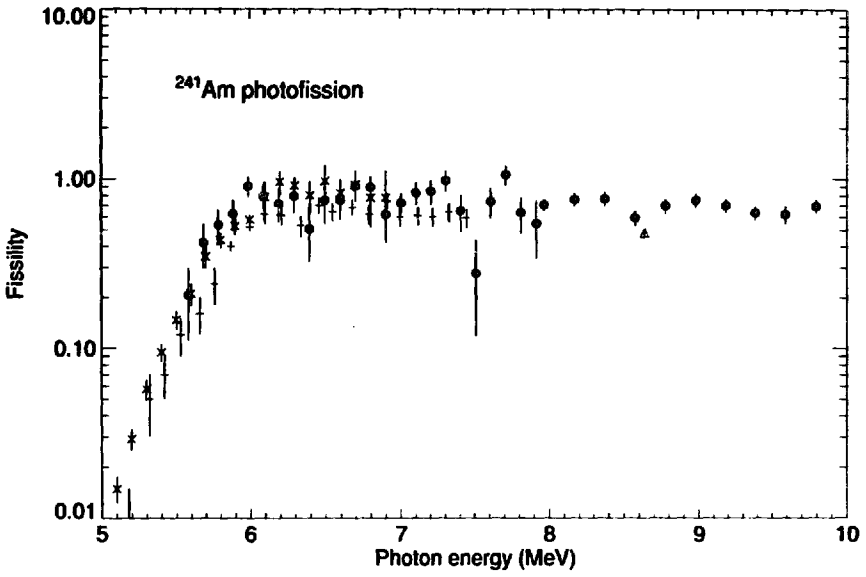

Fig. 2. Fissility of ^{241}Am. Solid circles, from present data; crosses, from Zhuchko *et al.* [3]); dashes, Back *et al.* [16]); triangle, Aleksandrov *et al.* [6]) at mean photon energy corresponding to 11.5 MeV endpoint energy.

In fig. 3 is shown the photoneutron cross section from the present experiment. The energy resolution is 300 keV and 500 keV below and above 8 MeV, respectively. Also shown are the data of Batij *et al.* [8]). The solid line is a fit to the two sets of data. Also shown for comparison are fits to the ^{237}Np and ^{239}Pu photoneutron cross sections of Berman *et al.* [5]). The anomalous narrowness of the ^{239}Pu cross section tends to confirm the suspicion from the negative-going cross section in fig. 7b of

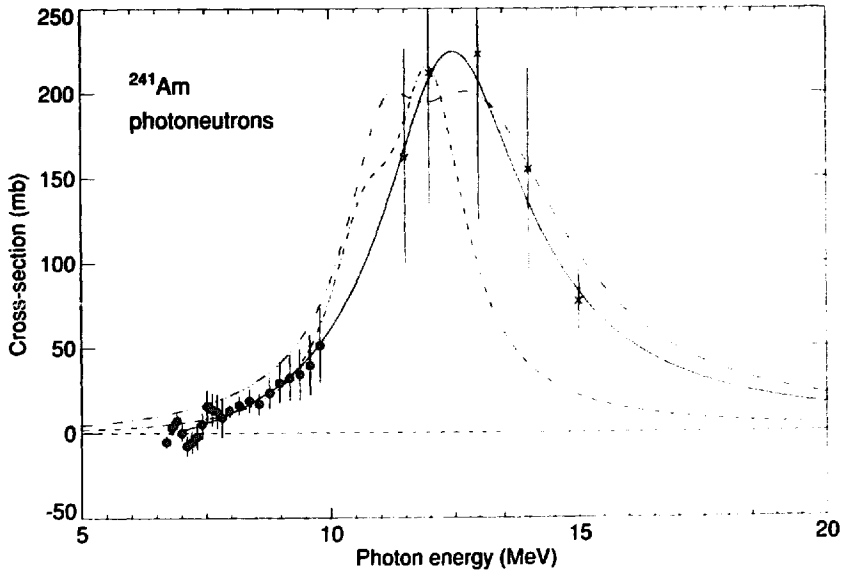

Fig. 3. Photoneutron cross section for ^{241}Am. Data: solid circles, present data; crosses, Batij *et al.* [8]). Curves: solid line, fit to all data shown; dash-dot and dash-triple-dot, fits to ^{239}Pu and ^{237}Np photoneutron cross sections respectively of Berman *et al.* [5]).

ref. [5]) that strength has been wrongly distributed amongst the (γ, n) and other channels for ^{239}Pu in ref. [5]).

The $\bar{\nu}$ values shown in fig. 4 are the results of fits to the summed multiplicity distributions as described in sect. 3. The values are assigned to mean photon energies each of which is obtained by folding together the photofission cross section and a bremsstrahlung spectrum with an endpoint energy equal to the mean of the two endpoint energies in each run. Also shown in fig. 4 is a two-piece linear fit. The slope of 0.059 ± 0.047 MeV^{-1} above 6.8 MeV is not inconsistent with the slope from general systematics of 1 in $\bar{\nu}$ for every ~8 MeV of excitation energy [18]), but below 6.8 MeV the slope is negative with a value -0.20 ± 0.04 MeV^{-1}. Such negative slopes have been seen before at low excitation energies [19-21]) and are presumably due to shell effects. However, no quantitative predictions of this negative slope region of $\bar{\nu}$ have been made, and this negative-slope feature would clearly benefit from further theoretical work. Also shown in fig. 4 are data from ^{243}Am from the reaction ^{242m}Am(n, f) [17]. The $\bar{\nu}$ data presented in ref. [17]) as a ratio to $\bar{\nu}$ for ^{235}U were multiplied by the ^{235}U evaluation of ref. [18]), shifted upwards in energy to correspond to excitation energy in ^{243}Am instead of incident neutron energy, and shifted vertically downwards to correspond to an ^{241}Am fissioning system assuming $d\bar{\nu}/dA = 0.1$ [ref. [22])] where A is the nuclear mass number. The dashed line is a fit to all the data of ref. [17]) which extend up to a much higher energy than is shown in fig. 4. The fact that the incident neutron energy must be positive sets the lower-energy limit of the data from ref. [17]) in fig. 4, and so fig. 4 makes the point well that the photonuclear

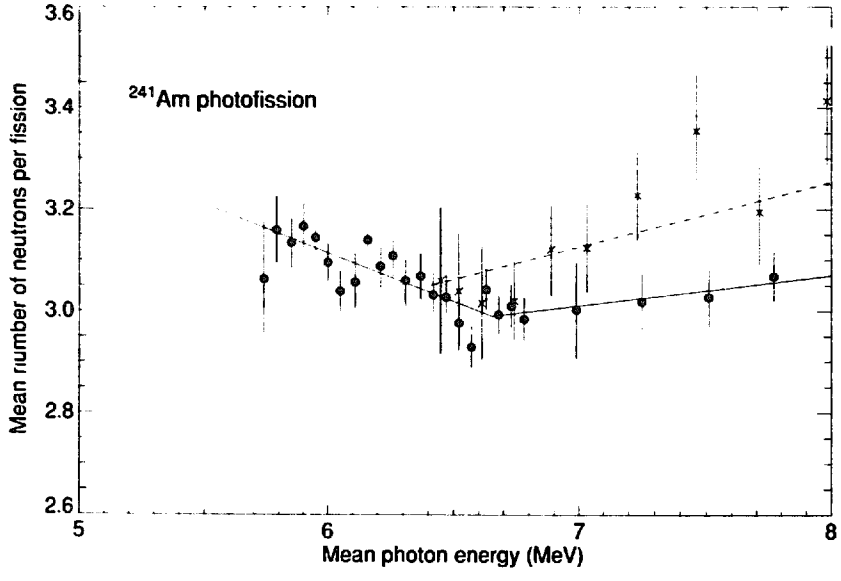

Fig. 4. Mean number $\bar{\nu}$ of neutrons per fission. Data: solid circles, present data at mean photon energies corresponding to bremsstrahlung spectra endpoint energies as discussed in the text; crosses, Howe *et al.* [17]) for ^{243}Am shifted to correspond to ^{241}Am as discussed in the text. Solid line, minimum-χ^2 two-piece linear fits to present data (slopes -0.20 ± 0.04 and 0.059 ± 0.047 MeV^{-1}); dashed line, linear fit to data (up to 30 MeV) of Howe *et al.*

probe is necessary to extend measurements of $\bar{\nu}$ into regions where the slope of $\bar{\nu}$ as a function of excitation energy could be negative.

5. Cross-section calculations and discussion

The photofission cross section is in general given by [23])

$$\sigma_{\gamma f}(E) = \sum_{lJ\pi} \left(\frac{\sigma^{l}_{\gamma a} \sum_{\nu} T^{\nu}_{f}(EJ\pi)}{\sum_{\nu} T^{\nu}_{f}(EJ\pi) + \sum_{\mu} T^{\mu}_{\gamma}(EJ\pi) + \sum_{\xi} T^{\xi}_{n}(EJ\pi)} \right), \tag{2}$$

where $\sigma^{l}_{\gamma a}$ is the photon-absorption cross section for multipole order l, T^{ν}_{f}, T^{μ}_{γ} and T^{ξ}_{n} are the fission, γ-ray and neutron transmission coefficients respectively and ν, μ and ξ are summed over all permissible fission, γ-ray and neutron emission channels respectively for the state $EJ\pi$ in the nucleus, where E is the photon energy or excitation energy, and J and π are the spins and parities of states in the excited nucleus. In order to use eq. (2) to calculate cross sections for comparison with the present photofission measurements, and in particular to investigate the possibility of structure in the photofission cross section at ~6 MeV, various approximations were made.

In the photofission cross-section calculations, E1 excitations were assumed to account for 98% of the interaction strength [23]), the remaining 2% being E2. The fission barriers corresponding to the fission channels ν are assumed to have the same double-humped shape made up of smoothly joined parabolic sections but are displaced in energy relative to one another. The direct penetrability of each fission barrier was calculated using an iterative procedure in which the potential barrier was divided into small steps and the Schrödinger wave equation was solved for each step following the method of Bjørnholm and Lynn [24]). A small imaginary component was added to the second well to simulate damping of flux by levels in this well. This flux is absorbed into the second well and can be re-emitted back into the fission channel. This absorbed flux is treated according to the method of Back *et al.* [25,26]) allowing K-mixing to occur [27]). The fission-channel barrier heights were inferred from quasi-particle calculations of Back [28]). The ground-state barrier heights and curvatures were taken from Bjørnholm and Lynn [24]). The continuum region was modelled using the complete-damping approximation [16,29,30]), and the fission-channel level density at each hump was assumed to have an exponential dependence [31]). For the γ-ray transmission coefficient only E1 decay in the first well was assumed, and the expression of Vandenbosch and Huizenga [23]) was used. The neutron transmission function was calculated in the black-nucleus approximation using a real square-well potential, and the level density of Gilbert and Cameron [32]) was used in the continuum for the $A-1$ nucleus. The E1 photon absorption cross section was approximated by the tail of the giant dipole resonance (GDR) [33,34]). (The E2 photon-absorption cross section was simply assumed to be 2% of the E1.)

The solid line in fig. 1 is the ^{241}Am(γ, f) cross section calculated * as described above but with no damping in the second well. It can be seen that there are resonances at 5.5 and 5.9 MeV. The long-dashed line shows the same calculation but with 220 keV gaussian smearing to represent the effects of the experimental energy resolution. The resonance at 5.9 MeV becomes a change in slope, but the peak at 5.5 MeV is still visible. The short-dashed line shows the effect of adding a 300 keV imaginary damping component to the potential in the second well. Although the peak at 5.5 MeV is still visible, the change in slope at 5.9 MeV has almost disappeared. This suggests that if the structure observed in the experimentally measured cross section at 6.1 MeV is due to a sub-barrier resonance, then the magnitude of the damping in the second well is certainly less than 300 keV. [Damping parameters smaller than 300 keV have been used in previous work [35].] Further high-resolution measurements between 5 and 7 MeV might help to establish whether the apparent structure at 6.1 MeV actually does exist.

6. Conclusions

The photofission cross section of ^{241}Am has been measured with better energy resolution than before. The first measurements of the mean number $\bar{\nu}$ of neutrons per fission and of the photoneutron cross section below 11 MeV have been made.

There is an indication of the presence of structure in the photofission cross section at ~6 MeV which, theoretical calculations suggest, might be due to resonances in the fission transmission function of the double-humped barrier. Such resonances are not normally expected to be seen in odd-A nuclei because of damping in the second well of the fission barrier. However, photofission measurements by Zhuchko *et al.* [3]) do indicate structure in other odd-A nuclei. Unfortunately, the data points in the photofission cross sections of Berman *et al.* [5]) for odd-A actinide nuclei are too widely spaced for any structure to be evident. Clearly there is a need for more detailed high-resolution measurements of photofission cross sections to be made in the threshold region of odd-A actinide nuclei such as ^{237}Np, ^{239}Pu and ^{241}Pu.

A negative-slope region below 6.8 MeV has been shown to be present in the $\bar{\nu}$ data. Further theoretical work is required to explain this feature quantitatively.

As far as a comparison is possible, the present photoneutron cross-section data are consistent with the data of Batij *et al.* [8]).

We should like to thank the Oak Ridge National Laboratory for the loan of the americium sample. We should also like to thank Dr. B.B. Back for supplying the results of quasi-particle calculations. In addition, we should like to acknowledge support from the Underlying Research Programme of the UK Atomic Energy Authority. Finally one of us (SJW) would like to acknowledge support from the UK Science and Engineering Research Council.

* This sudden change in slope of the cross section at 7 MeV is due partly to the bridging of the pairing gap and partly to the *ad hoc* way that the resonant and complete-damping calculations have been joined at this point.

References

1) Yu.B. Ostapenko, G.N. Smirenkin and A.S. Soldatov, Sov. J. Part. Nucl. **12** (1981) 454 [Fiz. Elem. Chastits At. Yadra **12** (1981) 1364]
2) V.V. Varlamov, B.S. Ishkhanov, M.E. Stepanov, V.V. Surgutanov, A.A. Khoronenko and A.P. Chernjaev, Photonuclear Data, Photofission of Nuclei 1952-1988, USSR Photonuclear Data Centre, Moscow (1989)
3) V.E. Zhuchko, Yu.B. Ostapenko, G.N. Smirenkin, A.S. Soldatov and Yu.M. Tsipenyuk, Sov. J. Nucl. Phys. **28** (1978) 602 [Yad. Fiz. **28** (1978) 1170]
4) I.S. Koretskaya, V.L. Kuznetsov, L.E. Lazareva, V.G. Nedorezov and N.V. Nikitina, Sov. J. Nucl. Phys. **30** (1979) 472 [Yad. Fiz. **30** (1979) 910]
5) B.L. Berman, J.T. Caldwell, E.J. Dowdy, S.S. Dietrich, P. Meyer and R.A. Alvarez, Phys. Rev. **C34** (1986) 2201
6) B.M. Aleksandrov, A.S. Krivokhatskii, L.E. Lazareva, V.G. Nedorezov, P.S. Soloshenkov and A.S. Sudov, Sov. J. Nucl. Phys. **43** (1986) 185 [Yad. Fiz. **43** (1986) 290]
7) A. Veyssière, H. Beil, R. Bergère, P. Carlos and A. Lepretre, Nucl. Phys. **A199** (1973) 45
8) V.G. Batij, V.Ya. Golovnya, I.Yu. Gorshkov, S.S. Kovalenko, O.I. Osetrov, A.N. Smirnov, G.F. Timoshevskij and S.V. Khlebnikov, 40th Conf. on Nuclear spectroscopy and nuclear structure, Leningrad, USSR, April 1990
9) J.E. Lynn, Contemp. Phys. **21** (1980) 483
10) S.J. Watson, Ph.D. Thesis (1990), University of Edinburgh (unpublished)
11) J.S. Pruitt and S.R. Domen, Determination of total X-ray beam energy with a calibrated ionisation chamber, NBS Monograph 48 (Washington, 1962)
12) E.W. Lees, B.H. Patrick and E.M. Bowey, Nucl. Instr. Meth. **171** (1980) 29
13) G. Edwards, D.J.S. Findlay and E.W. Lees, Ann. Nucl. Energy **8** (1981) 105
14) D.J.S. Findlay, Nucl. Instr. Meth. **213** (1983) 353
15) D.J.S. Findlay, N.P. Hawkes and M.R. Sené, Nucl. Phys. **A458** (1986) 217
16) B.B. Back, H.C. Britt, O. Hansen, B. Leroux and J.D. Garrett, Phys. Rev. **C10** (1974) 1948
17) R.E. Howe, J.C. Browne, R.J. Dougan, R.J. Dupzyk and J.H. Landrum, Nucl. Sci. Eng. **77** (1981) 454
18) F. Manero and V.A. Konshin, At. Energy Rev. **10** (1972) 637
19) J.T. Caldwell, E.J. Dowdy, R.A. Alvarez, B.L. Berman and P. Meyer, Nucl. Sci. Eng. **73** (1980) 153
20) J.W. Boldeman, W.K. Bertram and R.L. Walsh, Nucl. Phys. **A265** (1976) 337
21) J. Caruana, J.W. Boldeman and R.L. Walsh, Nucl. Phys. **A285** (1977) 217
22) D.C. Hoffman, 50 Years with nuclear fission, ed. J.W. Behrens and A.D. Carlson (Amer. Nucl. Soc., Illinois, 1989)
23) R. Vandenbosch and J.R. Huizenga, Nuclear fission (Academic Press, New York, 1973)
24) S. Bjørnholm and J.E. Lynn, Rev. Mod. Phys. **52** (1980) 725
25) B.B. Back, J.P. Bondorf, G.A. Ostroschenko, J. Pedersen and J. Rasmussen, Nucl. Phys. **A165** (1971) 449
26) B.B. Back, O. Hansen, H.C. Britt, J.D. Garrett, Phys. Rev. **C9** (1974) 1924
27) J.P. Bondorf, Phys. Lett. **B31** (1970) 1
28) B.B. Back, private communication (1990)
29) T. Ohsawa, Y. Shigemitsu, M. Ohta and K. Kudo, J. Nucl. Sci. Tech. **21** (1984) 887
30) D.L. Hill and J.A. Wheeler, Phys. Rev. **89** (1953) 1102
31) J.E. Lynn, Systematics for neutron reactions of the actinide nuclei, Harwell report AERE-R 7468 (1974)
32) A. Gilbert and A.G.W. Cameron, Can. J. Phys. **43** (1965) 1446
33) J.W. Knowles, W.F. Mills, R.N. King, B.O. Pich, S. Yen, R. Sobie, L. Watt, T.E. Drake, L.S. Cardman and R.L. Gulbranson, Phys. Lett. **B116** (1982) 315
34) P. Axel, Phys. Rev. **126** (1962) 671
35) H.X. Zhang, T.R. Yeh and H. Lancman, Phys. Rev. **C34** (1986) 1397